1

MODELING AND CONTROL OF LARGE CONVECTIVE FLOWS WITH TIME-DELAYS

Emmanuel WITRANT[1]* and Silviu-Iulian NICULESCU[2].

[1] *GIPSA-Lab, Université Joseph Fourier/CNRS, Grenoble, France.*
[2] *LSS-SUPELEC, CNRS, Gif-sur-Yvette, France.*

Summary. Large convective flows are involved in numerous applications with crucial real-time control objectives. Focusing on the - potentially time-varying - transport properties involved in the flow model and appropriate physical hypotheses, the aim of this paper is to propose a new modeling and model-based boundary control approach. Online estimation strategies are proposed to evaluate the time-varying transport coefficients. A mathematical equivalence is then obtained between the distributed model and a time-delay system, which is used to derive a feedback control law. The theoretical results are illustrated on simulations and on a mining ventilation benchmark.

* Corresponding author: `emmanuel.witrant@gipsa-lab.grenoble-inp.fr`

1 INTRODUCTION

Convective flows are present in many applications for which simplified models and feedback control strategies may be desired. For example, one may consider the recycling of burned gases in car engines, helium transport in cryogenic devices or airflows in ventilation systems (buildings, tunnels or mines). In such cases, detailed dynamic models and the use of computational fluid dynamics would not be suitable for reduced complexity and real-time objectives. *Space-averaged* models can be used to describe large and/or turbulent flows and analyzed to meet with the previous objectives.

Distributed time-delay systems provide a appealing alternative to the more classical physical models described by partial differential equations (PDE), especially to infer some global system properties with flow interconnections. The resulting functional differential equations (FDE) can describe some non-homogeneous transport phenomena with a greatly reduced number of variation laws. Furthermore, numerous research studies have been carried on the analysis and control of such systems (see for example [1, 2, 3]).

The purpose of this paper is to derive a time-delay approach for the modeling and control of large convective flows. Starting from a classical physical model, some hypotheses are first made according to the "large" flow property (on Euler equations and the coupling between the state variables) to derive a convective-resistive PDE model. The convection and resistance coefficients are time-varying (which allows for the consideration of non-homogeneous transport coefficients) and dedicated estimation methods are proposed, supposing that distributed flow measurements are available. A time-delay approach is then derived, using the method of characteristics, to express the PDE model as a FDE with a distributed delay kernel. This FDE is used to set a feedback control strategy with tracking objectives. The efficiency of the proposed method is finally illustrated on an airflow regulation problem associated with mining ventilation control.

2 LARGE CONVECTIVE AIRFLOWS

2.1 Physical model and hypotheses.

This section briefly summarizes the main results presented in [4], where a non-dimensional model was proposed to describe a large flow thanks to the bond graph approach. The flow is described by interconnected cells containing height-averaged values, which is equivalent to a control volume discretization (a single volume is used at each height). The flow dynamics is obtained for each cell by deriving a flow/effort model from Euler equation (see classical fluid dynamics textbooks such as [5] for a complete description):

$$\frac{\partial}{\partial t} \begin{bmatrix} \rho \\ \mathbf{M} \\ \rho E \end{bmatrix} + \nabla \cdot \begin{bmatrix} \mathbf{M} \\ \mathbf{M}^T \otimes \mathbf{V} + p\mathbf{I} \\ \mathbf{M}H \end{bmatrix} = \begin{bmatrix} 0 \\ 0 \\ \dot{q} \end{bmatrix}, \tag{1}$$

where ρ is the density, $\mathbf{M} = \rho\mathbf{V}$ ($\mathbf{V}$ being the flow speed) the momentum, p the pressure, E the energy (per unit mass), $\otimes$ the tensor product of two vectors, H the

total enthalpy and $\dot{q}$ is the rate of heat addition (see [6] for a precise description). This description is complemented with the perfect gas equation of state $p = \rho RT$, where R the specific gas constant and T the temperature. Considering a sufficiently large airflow, the following hypotheses can be made:

$H1$) in the momentum equation, the impulsive term is negligible compared to the pressure: $\rho v^2 << p$ and the dynamics is approximated with an algebraic relationship (i.e. Saint-Venant);

$H2$) only the static pressure is considered, implying that the kinetic energy term in the energy conservation equation is omitted: $H = E + p/\rho$;

$H3$) the gas is calorically perfect: $E = c_v T$, where $c_v = R/(\gamma - 1)$ ($\gamma = 1.4$) is the specific heat at constant volume.

2.2 Distributed pressure dynamics

For real-time control purposes, we are specifically interested in the pressure dynamics, which is the regulated variable. A dedicated model is obtained from $H1 - H3$ and (1) by expressing the energy equation in terms of pressure (perfect gas equation) as:

$$\frac{\partial \rho E}{\partial t} = -\frac{\partial}{\partial x}\left[M \cdot \left(E + \frac{p}{\rho}\right)\right] + \dot{q}$$

$$\Leftrightarrow \frac{\partial \rho c_v T}{\partial t} = -\frac{\partial}{\partial x}\left[\frac{M}{\rho} \cdot (c_v \rho T + p)\right] + \dot{q}$$

$$\Leftrightarrow \frac{\partial p}{\partial t} = -\frac{\partial}{\partial x}\left[\frac{M}{\rho} \cdot \left(1 + \frac{R}{c_v}\right)p\right] + \frac{R}{c_v}\dot{q}. \tag{2}$$

Note that the momentum can be obtained by implicit resolution of the Darcy-Weisbach equation, which then provides the dynamics of the density evolution. The energy losses are defined as pressure losses induced by the surrounding environnement:

$$\dot{q}(x,t)R/c_v = s(x,t) + r(t)p(x,t),$$

where $s(x,t)$ describes the losses due to flows leaving the main stream (sink term) and $r(t)$ denotes the friction losses on the boundaries. Both s and r are considered as known engineering parameters or estimated with appropriate algorithms, as detailed below.

Such a model can be used, for example, to describe a Poiseuille flow in a duct with outflows at specific (known) locations.

2.3 Control-oriented model and control problem

In order to design a model-based feedback controller, the model should depict the main tendencies and essential properties of the system dynamics. Indeed, the transport parameters estimation proposed in the next section and the feedback control strategy are expected to compensate the modeling error thanks to the sensors measurements. Our aim is then to infer the model architecture from the physics and identify suitable "free" parameters that will be provided by the estimation algorithm.

Consider the volume-averaged impact of the momentum and density on the pressure dynamics, with

$$\bar{M}(t) \doteq \frac{1}{\mathcal{V}} \oint_{\mathcal{V}} M(v,t)dv \quad \text{and} \quad \bar{\rho}(t) \doteq \frac{1}{\mathcal{V}} \oint_{\mathcal{V}} \rho(v,t)dv,$$

where $\mathcal{V}$ is the shaft control volume. Introducing the t and x subscripts to denote the time and space differentiations, respectively, the physical model (2) is then approximated with the control-oriented model:

$$\begin{cases} \tilde{p}_t = c(t)\tilde{p}_x + r(t)\tilde{p} + s(x,t), \\ \tilde{p}(0,\,t) = p_{in}(t) \end{cases} \tag{3}$$

where $c(t) \doteq -\bar{M}(t)/\bar{\rho}(t) \cdot (1 + R/c_v)$. The boundary condition is set by the inflow pressure $p_{in}(t)$.

Supposing that a proper system automation is available, the control problem can then be decomposed in two steps:

1. provide an estimation of the transport coefficients $c(t)$, $r(t)$ and possibly $s(x,t)$;
2. regulate the controlled input $p_{in}(t)$ according to some desired objective on the pressure distribution $\tilde{p}(x,t)$.

These estimation and control objectives are detailed in the next sections.

3 DISTRIBUTED MEASUREMENTS AND ONLINE PARAMETERS ESTIMATION

Distributed measurements (i.e. obtained thanks to a wireless sensor network deployed in the flow, see [7] for more details) are supposed to be available to set the control law. One of the main advantages is the possibility to constrain a simplified model according to the behavior of the flow through the time-varying parameters describing the convective, resistive and source terms.

3.1 Gradient descent approach

A classical identification problem is to find the set of free parameters ϑ in a given model that minimizes the difference between the measured and the estimated data. This is done in this section by choosing a cost function J which reflects the variance of the estimation error from a given set of measurements. Consider the general class of systems that write as:

$$p_t = d(t)p_{xx} + c(t)p_x + r(t)p + s(t)p_{ext}(x,t) \tag{4}$$

where $\vartheta(t) = \{c(t), d(t), r(t), s(t)\}$ denotes the convective, diffusive, resistive and source coefficients, respectively, and $p_{ext}(x,t)$ is a distributed source term of known (time-varying) location. The boundary conditions are given by $p(0,\,t) = p_0(t)$ and $p_x(L,\,t) = 0$, for $x \in [0,\,L]$. In order to obtain a real-time estimation algorithm, the cost function is defined as:

$$J(\vartheta, t) = \frac{1}{2} \int_0^x ||p_{meas}(\theta, t) - p(\vartheta, \theta, t)||_2^2 d\theta$$

where $p_{meas}(x, t)$ is the measured pressure distribution. The output error is then minimized for ϑ^* satisfying:

$$\vartheta^* = \arg\min_\vartheta J(\vartheta, t)$$

This optimization problem can be solved with a descent algorithm, using the sensitivity of $p(x, t)$ with respect to ϑ, expressed as $S(\vartheta, x, t) \doteq \partial p / \partial \vartheta$. The gradient writes as:

$$\nabla J(\vartheta, t) = - \int_0^x [p_{meas}(\theta, t) - p(\vartheta, \theta, t)]^T S(\vartheta, \theta, t) d\theta$$

and the optimal parameter ϑ^* is obtained by moving along the steepest slope $-\nabla J$ with a step α, which has to be small enough to ensure that $\dot{\vartheta} = -\alpha \nabla J(\vartheta)$ converges to ϑ^*. This step is chosen according to *Newton's method* and writes as $\alpha \doteq (\Psi J(\vartheta) + \upsilon I)^{-1}$, where υ is a positive constant introduced to ensure strict positiveness and $\Psi J(\vartheta)$ is the pseudo-Hessian, derived with the Gauss-Newton approximation as:

$$\Psi J(\vartheta, t) = \int_0^x S(\vartheta, \theta, t)^T S(\vartheta, \theta, t) d\theta$$

The sensitivity function evolution is computed with the ODE method by noticing that:

$$\frac{d}{dt} \left[\frac{\partial p}{\partial \vartheta} \right] = \frac{\partial}{\partial p} \left[c(t) p_x + d(t) p_{xx} + r(t) p \right] \frac{\partial p}{\partial \vartheta} + [p_x \quad p_{xx} \quad p \quad p_{ext}] \tag{5}$$

Remark 1. The convergence speed of the algorithm is inversely proportional to the design parameter υ but choosing this parameter too small may create some oscillations in the algorithm (numerical instabilities).

3.2 Observer-based estimation

The parameter estimation problem can also be solved thanks to the observer-based approach described in [8], where it is supposed that the distributed dynamics is affine in the identified parameter ϑ. The main result of this work is synthesized in the following theorem.

Theorem 1 ([9]). *Consider the general class of systems described by:*

$$\begin{cases} p_t = \mathcal{A}(p, p_x, p_{xx}, u, \vartheta)\vartheta \\ a_1 p_x(0, t) + a_2 p(0, t) = a_3 \\ a_4 p_x(L, t) + a_5 p(L, t) = a_6 \end{cases} \tag{6}$$

where p is the state, u a known exogenous input, $\vartheta \in \mathbb{R}^M$ denotes a set of time-varying parameters, $\mathcal{A}(p, p_x, p_{xx}, u, \vartheta) \in \mathbb{R}^{1 \times M}$ sets the input-to-state relationship and a_i are scalar real coefficients. The estimated state $\hat{p}(x, t)$ converges exponentially to $p(x, t)$ in the $\mathcal{L}_2$ sense and:

$$||p(x,t) - \hat{p}(x,t)||_2^2 = e^{-2(\gamma+\lambda)t}||p(x,0) - \hat{p}(x,0)||_2^2$$

where $||\cdot||_2$ denotes the $\mathcal{L}_2$ norm and γ, λ are positive scalar parameters, if:

$$\begin{cases} \hat{p}_t = \mathcal{A}(\hat{p}, \hat{p}_x, \hat{p}_{xx}, u, \hat{\vartheta})\hat{\vartheta} + \gamma(p - \hat{p}) \\ a_1\hat{p}_x(0,t) + a_2\hat{p}(0,t) = a_3 \\ a_4\hat{p}_x(L,t) + a_5\hat{p}(L,t) = a_6 \\ \hat{\vartheta} = \mathcal{A}(\hat{p}, \hat{p}_x, \hat{p}_{xx}, u, \hat{\vartheta})^\dagger[p_t + \lambda(p - \hat{p})] \end{cases} \quad (7)$$

where $A^\dagger$ is the Moore-Penrose inverse of A.

Example 1. The accuracy of the proposed estimation methods is evaluated on a model where the transport parameters only depend on time. More precisely, consider (4) with the inputs ($p_0(t)$ and $p_{ext}(x,t)$) depicted in Figure 1 and $L = 1000$. The transport parameters (real and estimated) are presented in Figure 2 for both estimation methods.
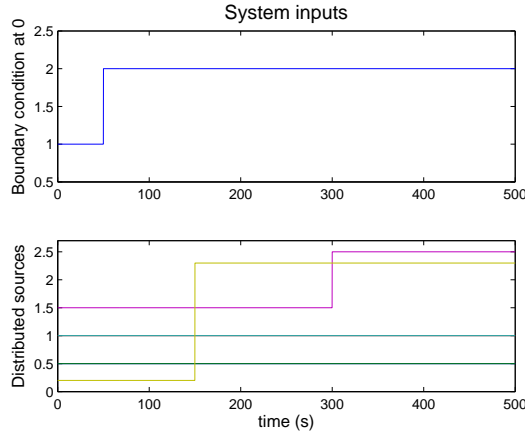

Fig. 1   Boundary condition and distributed pressure losses for the ideal case (4).

It can be noticed that the gradient-based approach may have some difficulties to decouple the variations associated with each transport phenomena (impact of the convection on the other terms) but provides a satisfying mean estimate. The observer-based method is more tractable and efficient in terms of decoupling the parameters effects but should be coupled with an appropriate filter to remove the impulses (induced by the inputs steps and re-appearing with a memory effect). This approach is more suited for real-time objectives as the number of discretized dynamics to compute $\hat{p}$ is the same as p (while the sensitivity computation necessitates the square of the dimension of p).
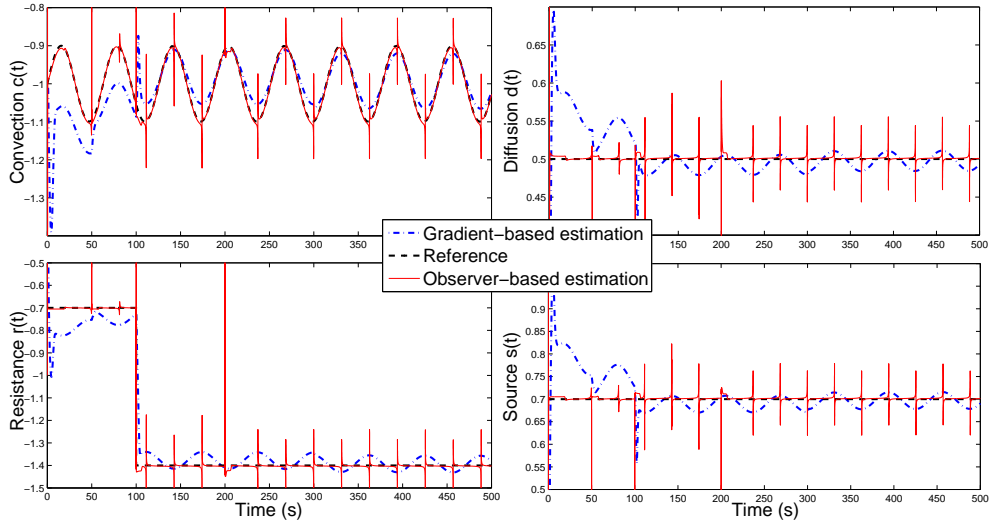
Fig. 2 Transport parameters estimation for the ideal case (4).

4 TIME-DELAY FORMULATION

While diffusion tends to stabilize the system, the convective effect is the main source of instability and/or poor closed-loop performance. Achieving a boundary control of the distributed model would involve large computation capabilities. This motivates the specific modeling approach presented in this section, where it is shown that a convective-resistive process can be associated with a time-delay model that do not involve the resolution of the initial PDE.

4.1 PDE model

Consider some generic (density, concentration, pressure) variable $p(\ \cdot,\ \cdot)$ depending on two independent variables t (time) and x (space) described by the PDE:

$$p_t(x,t) - c(t)p_x(x,t) = r(t)p(x,t), \tag{8}$$

where $c(t)$ and $r(t)$ denote appropriate speed and rate, respectively. It is assumed that these variables depend only on the (time-) variable t (volume-averaged model).

If this PDE is used to describe the evolution of some physical quantity inside some generic compartment, then the boundary condition (BC) can be given by:

$$p(0,t) \doteq u(t),$$

where u denotes some control (law) at the "input" ("entry") of the compartment. The initial condition (IC) can be given by:

$$p(x,0) \doteq \psi(x),$$

where ψ is an appropriate (differentiable) function and $x \in [0, L]$. Here $L > 0$ denotes a generic length of the (still generic) compartment.

4.2 Method of characteristics

Define a new variable ξ by integrating $p(x, t)$ over the interval $[0, L]$. The variable ξ can describe, for instance, an average behavior of the generic $p(\cdot, \cdot)$, that is:

$$\xi(t) \doteq \int_0^L p(\eta, t)d\eta.$$

Thus, (8) rewrites as:

$$\frac{d}{dt}\xi(t) \doteq -c(t)\left[u(t) - p(x, t)\right] + r(t)\xi(t), \tag{9}$$

which is nothing else than an ODE in the new variable ξ. However, we need to rewrite this last ODE by avoiding the use of $p(x, t)$ and this can be done by using the *method of characteristics*.

Introduce now a new *independent* variable θ such that $p(\theta) \doteq p(x(\theta), t(\theta))$. It is easy to see that:

$$\frac{dp}{d\theta} \doteq \frac{\partial p}{\partial t} \cdot \frac{dt}{d\theta} + \frac{\partial p}{\partial x} \cdot \frac{dx}{d\theta},$$

and by identifying:

$$\frac{dt}{d\theta} \doteq 1, \;\; \frac{dx}{d\theta} \doteq -c(t)$$

it follows that $p(\cdot)$ is described by the ODE (in the new variable θ):

$$\frac{dp}{d\theta} \doteq r(t)p.$$

Simple integrations lead to:

$$t(\theta) \doteq t_0 + \theta \qquad (t_0 = t(0)), \tag{10}$$

$$x(\theta) \doteq x_0 - \int_0^\theta c(\eta)d\eta \qquad (x_0 = x(0)), \tag{11}$$

$$p(\theta) \doteq p_0 \cdot \exp\left(\int_0^\theta r(t(\eta))d\eta\right) \qquad (p_0 = p(0)). \tag{12}$$

Now the plane defined by the variables t and x can be separated in *two regions* by the curve, assumed sufficiently regular, corresponding to the system's evolution starting from the origin $\mathcal{O} = (0, 0) \mapsto \mathcal{C}_\mathcal{O}$ and parameterized as follows:

$$\mathcal{C}_\mathcal{O} \doteq \left\{(t, x): \;\; t(\theta) = \theta, \;\;\; x(\theta) = -\int_0^\theta c(\eta)d\eta, \;\;\; \forall \theta \in [0, \theta_f]\right\},$$

where θ_f corresponds to:

$$L \doteq -\int_0^{\theta_f} c(\eta)d\eta.$$

Denote $\mathcal{R}_+$ ($\mathcal{R}_-$) the region situated above (below) the curve $\mathcal{C}_{\mathcal{O}}$ in the parameter space defined by (x, t). Thus, it seems clear that the solutions have different forms if located in $\mathcal{R}_+$ or $\mathcal{R}_-$. Based on the form of (12), we need to find some expression of p_0 as a function of the corresponding parameters in order to define properly $p(L, t)$.

- 1st case – $(x_0, t_0) \in \mathcal{R}_+$: Based on the definition of the partition, it makes sense to consider $t_0 = 0$, and thus $t(\theta) = \theta$ and $x(\theta)$ given by (11) with $0 < x(0) < L$. Using the IC, this leads to:

$$x_0 = \psi \left(x + \int_0^t c(\eta) d\eta \right),$$

  and thus:

$$p(L, t) \doteq \psi \left(L + \int_0^t c(\eta) d\eta \right) exp \left(\int_0^t r(\eta) d\eta \right),$$

  where we used the dependence of r on the parameter η as shown by (11).

- 2nd case – $(x_0, t_0) \in \mathcal{R}_-$: By similarity to the previous case study, $x_0 = 0$, and $t(\theta) = t_0 + \theta$. From the BC, $p_0 = u(t - \theta)$. Now, we need to find θ. This can be done, *implicitly*, by using $x(\theta)$ and an appropriate change of variables as, for example:

$$x(\theta) = -\int_0^\theta c(t(\eta)) d\eta = -\int_0^\theta c(t_0 + \eta) d\eta = -\int_{t_0}^{t_0+\theta} c(\eta) d\eta$$

  Using the standard heterogeneity assumption:

$$L = -\int_0^{\theta_f} c(\eta) d\eta = -\int_{t-\theta_f}^t c(\eta) d\eta,$$

  we have:

$$p(L, t) \doteq u(t - \theta_f) exp \left(\int_0^{\theta_f} r(\eta) d\eta \right).$$

In conclusion, the *method of characteristics* leads to:

$$p(L, t) \doteq \begin{cases} \psi \left(L + \int_0^t c(\eta) d\eta \right) exp \left(\int_0^t r(\eta) d\eta \right), \text{ if } (t, x) \in \mathcal{R}_+, \\ u(t - \theta_f) exp \left(\int_0^{\theta_f} r(\eta) d\eta \right), \qquad \text{if } (t, x) \in \mathcal{R}_-. \end{cases} \tag{13}$$

Since our main interest is related to long time behavior (stability, etc.), it seems clear that we are concentrating only on the region $\mathcal{R}_-$, as it includes the "time"-axis. Note that this expression directly expresses the fact that a given input is delayed by θ_f (convection effect) and attenuated by r (resistive effect).

4.3 Delay differential equation

A simple substitution of the corresponding $p(L, t)$ in (9) leads to the following ODE:

$$\frac{d}{dt}\xi = -c(t)\left[u(t) - u(t-\theta_f)exp\left(\int_0^{\theta_f} r(\eta)d\eta\right)\right] + r(t)\xi(t). \qquad (14)$$

Under the "strong" assumption that r is *constant*, we get:

$$\dot{\xi}(t) = -c(t)\left[u(t) - u(t-\theta_f)e^{r\theta_f}\right] + r\xi(t),$$

that can be easily interpreted as a DDE. Finally, in the case when $c(t)$ is also *constant*, some straightforward manipulations lead to a simpler DDE of the form:

$$\dot{\xi}(t) = -c\left[u(t) - u(t+L/c)e^{-rL/c}\right] + r\xi(t). \qquad (15)$$

It is interesting to observe the way the parameter c "enters" in the DDE (15). More precisely, we will have the *delay* $\theta = -L/c$ depending on some *parameter*.

Example 2. In order to investigate the efficiency of the time-delay model, consider Example 1 with:

$$c(t) = -10 + \cos(0.1t)$$
$$r(t) = -0.007 \text{ if } 0 \leq t \leq 300, \ r(t) = -0.1 \text{ if } t > 300$$
$$d(t) = s(t) = 0.001$$

The accuracy of the time-delay model is investigated by comparing the actual value of $p(L,t)$ with its estimate (supposing a slow variation of the transport parameters):

$$\theta_f(t) \approx -L/c(t)$$
$$\hat{p}(L,t) = p(0, t-\theta_f)e^{\mathcal{I}(t,\theta_f)}$$

where $\mathcal{I}(t,\theta_f)$ is the numerical approximation of $\int_{t-\theta_f}^t r(\eta)d\eta$. Note that the computation of $\mathcal{I}$ necessitates specific care when set in a feedback control setup [10]. It is simply implemented here using the trapezoidal rule with one and two intervals, denoted respectively as $\mathcal{I}_1$ and $\mathcal{I}_2$. The simulation results are presented on Figure 3.

After an initialization time approximately equal to θ_f ($\approx 100\,s$) the time-delay model provides a satisfying averaged approximation of $p(L,t)$. The variations in the convective term appear more strongly in $\hat{p}(L,t)$ than in $p(L,t)$. As expected, a difference between the responses obtained with $\mathcal{I}_1$ and $\mathcal{I}_2$ can be observed during a time θ_f after a variation of $r(t)$. A precise discretization of the integral term may be necessary if $r(t)$ has large variations (i.e. if the sinks are considered as resistive dissipation).

5 FEEDBACK CONTROL

Consider the reference tracking problem for the average distributed pressure:

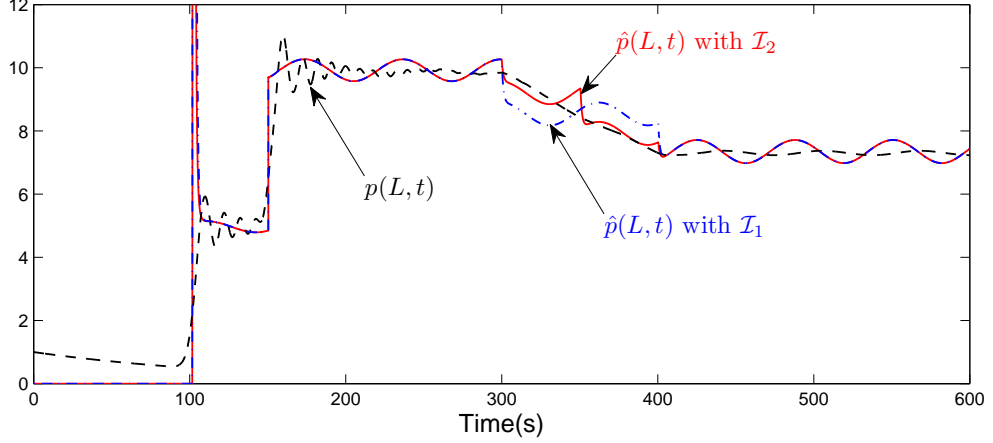$$\bar{p}(t) = \frac{1}{L}\int_0^L p(x,t)dx$$

Fig. 3 Approximation of the end value thanks to the time-delay approach.

Denoting as $\bar{p}_r(t)$ the reference average pressure, the control problem can be formulated as finding $p(0, t) = u(t)$ such that (fixed point theorem):

$$\dot{\bar{p}}(t) - \dot{\bar{p}}_r(t) + \lambda(\bar{p}(t) - \bar{p}_r(t)) = 0 \qquad (16)$$

where $\lambda > 0$ is a control tuning parameter. For simplicity, a step reference trajectory is chosen (constant $\bar{p}_r$), which implicitly means that a trajectory of a first order system is supposed to be achievable for $\bar{p}$. This is motivated by the first order nature of the PDE and may be refined depending on the application. Considering that convection and friction are the main flow effects that need to be compensated and according to (14), the following FDE is obtained:

$$\dot{\bar{p}}(t) = -\frac{c(t)}{L} \left[u(t) - u(t - \theta_f)exp\left(\int_0^{\theta_f} r(\eta)d\eta \right) \right] + r(t)\bar{p}(t).$$

Substituting in (16) provides the definition of the control law as:

$$-\frac{c(t)}{L} \left[u(t) - u(t - \theta_f)exp\left(\int_0^{\theta_f} r(\eta)d\eta \right) \right] + r(t)\bar{p}(t) + \lambda(\bar{p}(t) - \bar{p}_r) = 0$$

$$\Leftrightarrow u(t) = \frac{L}{c(t)} \left[r(t)\bar{p}(t) + \lambda(\bar{p}(t) - \bar{p}_r) \right] + u(t - \theta_f)exp\left(\int_0^{\theta_f} r(\eta)d\eta \right)$$

$$\Leftrightarrow u(t) = \frac{L}{c(t)} \left[r(t)\bar{p}(t) + \lambda(\bar{p}(t) - \bar{p}_r) \right] + p(L, t) \qquad (17)$$

where the last equality is obtained from (13). The feedback control law is then set according to (17) using the averaged distributed measurements $\bar{p}$ and the end pressure measurement $p(L, t)$. The averaged distributed pressure converges exponentially towards $\bar{p}_r$ according to (16) as:

$$|\bar{p}(t) - \bar{p}_r| = |\bar{p}(0) - \bar{p}_r|e^{-\lambda t}$$

Example 3. Setting the proposed control law with $\bar{p}_r = 1$ on the test case considered in Example 2, we obtain the controlled input and tracking error depicted on Figure 4. This result illustrates the efficiency of the proposed approach and its ability to compensate the transport properties variations for the regulation objective. The input oscillations are induced by the supposed first order trajectory for $\bar{p}(t)$ that is not fully met, but the tracking error is nevertheless rather satisfying.
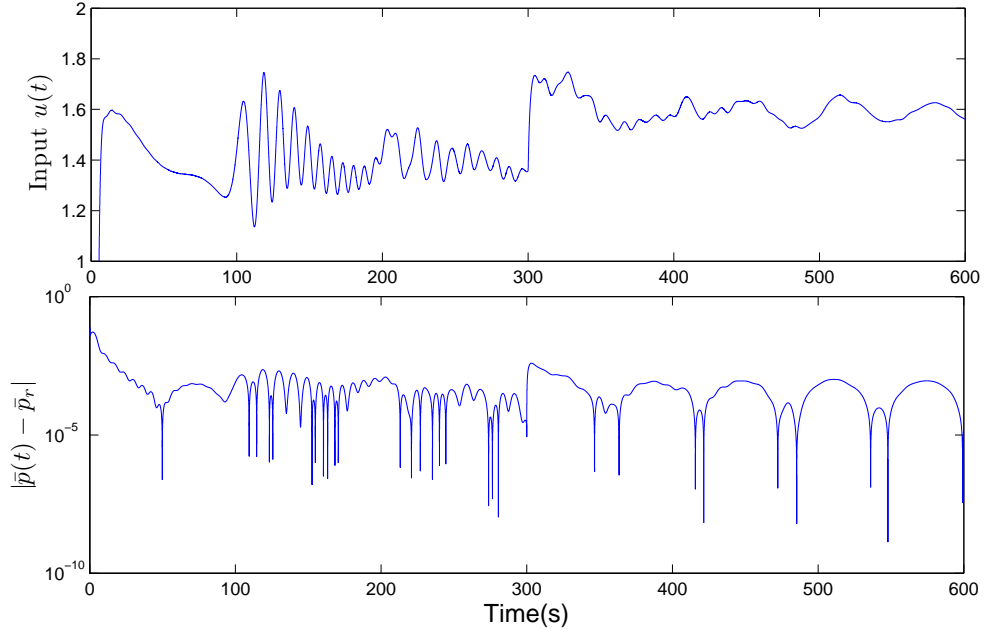

Fig. 4   Controlled input and tracking error.

6 APPLICATION TO MINING VENTILATION

Mining ventilation is an example of a large scale system with high environmental impact where a model-based control strategy can be of prime industrial interest. Indeed, as much as 50 % of the energy consumed by ore extraction goes into ventilation. The proposed model-based control strategy is now applied to this illustrative problem.

6.1 Process overview

The mine ventilation topology is depicted in Figure 5. It is achieved by a turbine and a heater connected on the surface to a deep pit (vertical shaft) that conducts
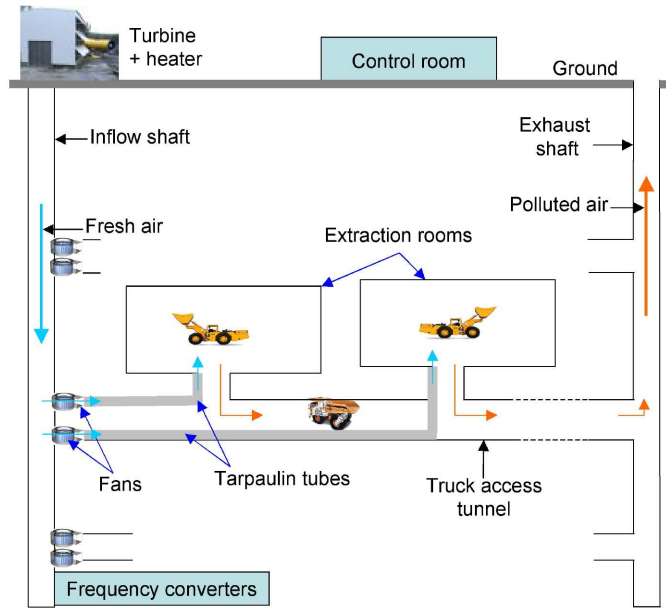
Fig. 5 Airflows in an underground mine.

the airflow to the extraction levels. The heater is introduced (in winter time at least) to avoid freezing in the upper part of the shaft and the air is cooled down at high depths (more than 1000 meters) because of the geothermal heating effect. From the deep pit, fans located at each extraction level pump fresh air to the extraction rooms via tarpaulin tubes. Bad quality air is naturally driven by the pressure gradient and flows from the extraction rooms back to the exhaust ventilation shaft (similar but separate from the inflow ventilation shaft).

From a control point of view, the regulation problem can be divided in two parts:

1. air quality regulation in the extraction rooms thanks to the fans and chemical sensors located in the rooms;
2. pressure regulation in the deep pit thanks to the ground turbine control and distributed sensors within the shaft.

The mine automation, communication network, historical background on real-time control and closed-loop control strategies for the second problem are detailed in [8]. The efficiency of these control strategies strongly depends on the available pressure in the vertical shaft (first problem), which is where the present results apply.

6.2 Simulation results

The proposed control approach is tested on the simulator presented in [4], where a non-dimensional (volume-averaged) model was derived thanks to a bond graph approach. This mine ventilation simulator is constructed based on the flow description and the fans models proposed in [11]. The deep pits (inflow and exhaust) are both discretized

with 28 control volumes and we consider three extraction levels. Airflow sinks are induced by the fans located at each level: the 1st level fan is not used (natural airflow), the 2nd one is operated at $1000\,s$ ($150\,\mathrm{rpm}$) and the 3rd runs continuously ($200\,\mathrm{rpm}$). The turbine and fans regulation is done by setting their rotational speed. Flow speed, pressure and temperature can be measured in each control volume. This simulator is used in the next sections to illustrate the estimation and control strategies. It may also be considered in the futur to develop virtual sensing capabilities in real-time operation schemes.

The control algorithm is set as follows. First, the convective and resistive behaviors are estimated thanks to the observer-based approach with the dynamics:

$$\begin{cases} \hat{p}_t = \mathcal{A}(\hat{p}, \hat{p}_x, \hat{\vartheta})\hat{\vartheta} + \gamma(p - \hat{p}) \\ \hat{p}(0, t) = u(t) \\ \hat{\vartheta} = \mathcal{A}(\hat{p}, \hat{p}_x, \hat{\vartheta})^{\dagger}[p_t + \lambda(p - \hat{p})] \end{cases}$$

where $\hat{\vartheta}(t) \doteq [\hat{c}(t),\ \hat{r}(t)]$ and $p(t)$ is a vector containing the pressures in the 28 control volumes (the previous equation is discretized at the measurements locations with a Lax-Wendroff scheme).

Secondly, the control law (17) is set as:

$$u(t) = \frac{L}{\hat{c}(t)}\left[\hat{r}(t)\bar{p}(t) + \lambda(\bar{p}(t) - \bar{p}_r)\right] + p(L, t)$$

where $\hat{c}(t)$ and $\hat{r}(t)$ are obtained according to the previous estimation, $\bar{p}(t)$ is the averaged distributed measurements and $p(L, t)$ is the pressure measured at the bottom of the shaft. The turbine rotation speed is regulated according to a PI control law that tracks the turbine output pressure $p(0, t)$ according to the reference $u(t)$.

Setting the desired average pressure $\bar{p}_r = 1.1\,hPa$, $p(0, t)$ and $u(t)$ are obtained as presented on Figure 6. The pressures in the tarpaulin tubes are depicted in Figure 7, for each exhaust level. While the closed-loop system tends to have an oscillatory behavior and is sensible to the initial conditions (this could be reduced by tuning the estimator parameters more precisely), the objectives in terms of exponential convergence of the tracking error are clearly met. The good compensation of the unplanned exhausts illustrates the robustness of the approach with respect to the modeling errors. Considering the pressures in the tarpaulin tubes, the proposed approach ensures an appropriate pressure (larger than the atmospheric one) for the extraction rooms.

CONCLUSIONS

The problem of modeling large convective flows was considered in this work. A physical analysis of these particular flows was first used to derive a space-averaged model, which has the structure of a convective-resistive transport system. Supposing that distributed measurements of the flow properties are available, estimation methods allowing for the online identification of time-varying parameters were proposed and compared. Some mathematical analysis was then introduced to propose a time-delay
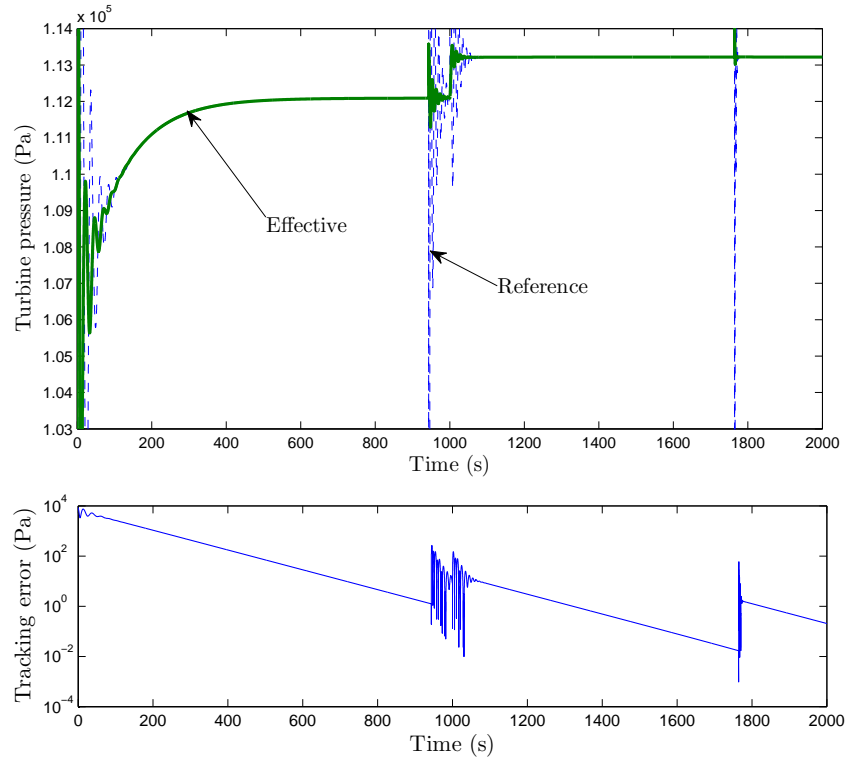
Fig. 6   Reference and effective turbine output pressure (top) and feedback tracking error (bottom).

model (FDE) from the initial PDE dynamics. A model-based feedback control strategy that fulfils a reference tracking objective on the FDE was finally set. Simulation results and application to a mining ventilation control benchmark illustrate the performances and limitations of the theoretical results.

ACKNOWLEDGEMENT

REFERENCES

1. L. Dugard and E. Verriest (Eds), *Stability and Control of Time-delay Systems*, ser. Lecture Notes on Control and Information Sciences.   New York: Berling-Verlag, 1997,
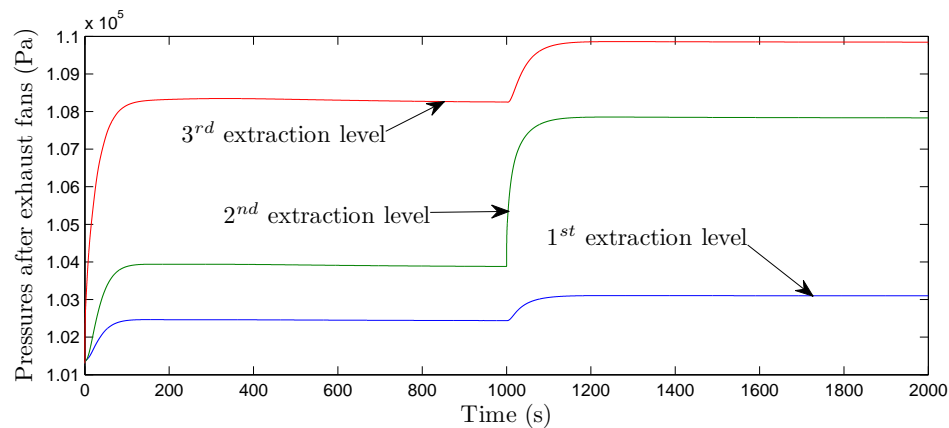
Fig. 7   Pressures provided to the extraction rooms at the three levels.

vol. LNCIS 228.

2. K. Gu, V. L. Kharitonov, and J. Chen, *Stability and robust stability of time-delay systems.* Boston: Birkhäuser, 2003.

3. W. Michiels and S.-I. Niculescu, *Stability and stabilization of time-delay systems. An eigenvalue based approach*, ser. Advances in Design and Control. Philadelphia: SIAM Publications, 2007, no. 12.

4. E. Witrant, K. Johansson, and the HynX team, "Air flow modelling in deep wells: application to mining ventilation," in *Proc. of the IEEE Conference on Automation Science and Engineering (CASE 2008)*, Washington DC, USA, Aug. 2008.

5. C. Hirsch, *Numerical Computation of Internal & External Flows: the Fundamentals of Computational Fluid Dynamics*, 2nd ed. Butterworth-Heinemann (Elsevier), 2007.

6. J. Brown, A. Vardy, and A. Tijsseling, "Response of wall heat transfer to flows along a cylindrical cavity and to seepage flows in the surrounding medium," Eindhoven: Technische Universiteit Eindhoven, Tech. Rep., 2005. [Online]. Available: ftp://ftp.win.tue.nl/pub/rana/rana05-35.pdf

7. C. Fischione, C. Rinaldi, L. Pomante, F. Santucci, and S. Tennina, "Mining ventilation control: Wireless sensing, communication architecture and advanced services," in *Proc. of the IEEE Conference on Automation Science and Engineering*, Washington DC, USA, Aug. 2008.

8. E. Witrant, A. D'Innocenzo, G. Sandou, F. Santucci, M. Di Benedetto, A. Isaksson, K. Johansson, S. Niculescu, S. Olaru, E. Serra, S. Tennina, and U. Tiberi, "Wireless ventilation control for large-scale systems: the mining industrial case," *International Journal of Robust and Nonlinear Control*, vol. 20, no. 2, pp. 226–251, 2010.

9. E. Witrant and N. Marchand, *Mathematical Problems in Engineering, Aerospace and Sciences*, ser. Scientific Monographs and Text Books. Cambridge Scientific Publishers, 2010, ch. Modeling and Feedback Control for Air Flow Regulation in Deep Pits, to appear.

10. S. Mondié and W. Michiels, "Finite spectrum assignment of unstable time-delay systems with a safe implementation," *IEEE Transactions on Automatic Control*, vol. 48, no. 12, pp. 2207–2212, Dec. 2003.

11. V. Talon and S. Cstric, "Engine control model based design with achille library," *E-COM: Rencontres scientifiques de l'IFP*, pp. 33–51, Oct. 2006.